AD-A033 375   ROYAL AIRCRAFT ESTABLISHMENT FARNBOROUGH (ENGLAND)   F/G 22/2
A CONING ANGLE SENSOR AND A SUN ANGLE SENSOR FOR USE IN SPINNIN--ETC(U)
JUN 76   C T FARR
UNCLASSIFIED   RAE-TR-76076   DRIC-BR-53656   NL

1 OF 1
ADA033375

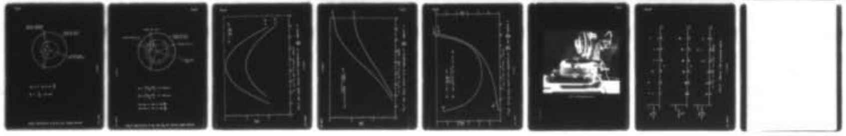

END

DATE
FILMED
2-77

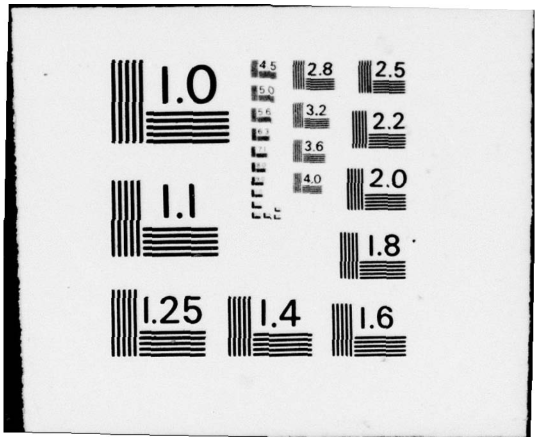
1.0
4.5
5.0
5.6
6.3
2.8
3.2
3.6
4.0
2.5
2.2
2.0
1.1
1.8
1.25
1.4
1.6

UDC 629.19.052.31 : 629.195 : 533.6.013.7 : 629.19.077.31

(18) DRIC

(14) RAF-TR-76076

(19) BR-53656

ROYAL AIRCRAFT ESTABLISHMENT

(9) Technical Report 76076

Received for printing 18 June 1976

(6) A CONING ANGLE SENSOR AND A SUN ANGLE SENSOR FOR USE IN SPINNING SATELLITES.

by

(10) C. T. Farr (11) Jun 76

(12) 20p.

SUMMARY

A coning angle sensor, using a new precision sun slit, has been developed for the UK6 satellite to measure the actual spin axis direction of the spacecraft with respect to body axes using the sun as an external reference. This paper describes the theory and construction of this sensor together with a complementary inclined slit sensor which is used to measure the angle of the satellite spin axis with respect to the satellite sun line.

This Report is based on a paper which was presented at the Fifth Annual Conference on Space Optics organised by CNES in Marseilles on 14-17 October 1975.

Departmental Reference: Space 508

310 450

LB

CONTENTS

C013477-78

1 INTRODUCTION

Failure of a spin stabilised spacecraft to rotate about its nominal spin axis, due to imperfect balancing or structural distortion of the satellite, can lead to loss of information from axially viewing experiments due to the coning motion of their fields of view.

The paper describes two sensors developed for use on spinning satellites which use a new precision sun slit detector developed under contract by Integrated Photomatrix Ltd., Dorchester. The two sensors are complementary insofar as one measures the angle of the sun relative to the nominal spin axis of the satellite, whilst the other determines the actual spin axis position of the spacecraft with respect to body axes, using the sun as an external reference. An iterative correction procedure can then be applied between the two sets of sensor data to obtain an improved estimate of Ψ , the sun to spin axis angle and this in turn to recalculate θ_s , the error between the nominal and actual spin axis of the vehicle.

2 DESCRIPTION OF PRECISION SLIT DETECTOR

The precision sun slit used in both the sun angle and coning angle sensors is shown in Fig. 1. The detector consists of a fused silica block on the front surface of which an entrance slit 500 microns wide has been formed by photolithographically etching a thin mask of chromium. The chromium mask also acts as an optical reference surface for measurement of the alignment of the sensor with respect to the satellite. Mounted on the rear face of the fused silica block, in a plane parallel to the reference face and normal to the entrance slit, is a linear array of *five* silicon photodiodes, each diode being approximately 127μ square and separated by a 12μ spacing. During manufacture of the detector the arrays are selected so that the two outer diodes, (i.e. diodes 1 and 5), have their responses matched to within ±5%. The array is positioned transverse to the slit so that a null is obtained from the differenced outputs of diodes 1 and 5 when sunlight incident on the slit lies within ±2 minutes of arc of a plane containing the centre line of the slit and the normal to the reference face. The difference signal, after limiting to produce logic signal levels of plus four and minus four volts, is connected to a 'gate' which inhibits the sensor output until a 'sun presence signal' is produced by the three central diodes which are all electrically connected together. Thus by choosing a suitable threshold for the sun presence signal, spurious triggering of the sensor output by albedo effects is eliminated. In the case of the detectors developed for the UK6 satellite the geometry of the slit and fused silica block have been designed to give a sensor field of view of $\pm 70^{o}$. To allow for the reduction in illumination of the detector near the edges of the field of view and for losses due to reflections occurring at the various optical interfaces, a threshold level of 20% of full sunlight has been chosen. With this value of threshold the field of view transverse to the plane defined by the slit and a normal to the reference face is approximately $\pm 1.5^{o}$.

The technique of bonding the detector array to a fused silica block with the entrance slit etched onto the front surface was adopted with the aim of obtaining maximum stability between the entrance slit and diode array and thus obtaining a highly stable sun detection plane for the sensor. All measurements so far carried out have indicated that this aim has been achieved. Temperature tests in the range $-30^{o}C$ to $+50^{o}C$ have shown changes in the null plane of the detector to be less than 1 minute of arc over the whole of the sensor field of view. The design also has the added advantage that a highly accurate and reproducible slit can be obtained at a fraction of the cost which would be incurred if the same accuracy was to be achieved using normal machining practice.

3 PRINCIPLES OF OPERATION

The two sensors, the sun angle and coning angle sensor, have been combined into a single instrument shown in Fig.2. Although their principles of operation are basically the same these are best understood by considering the sun angle sensor which comprises a single slit with the detector plane inclined to the actual spin axis of the satellite at a fixed angle θ .

Fig.3 shows a single slit PP' with the plane defined by the slit and its detector inclined at an angle θ to the actual spin axis of the satellite xx'. For a given sun to spin axis angle Ψ , successive transits of the slit by the sun occur for angular rotations ϕ of the satellite about its spin axis. By applying simple trigonometry to this figure, for fixed angles of θ and Ψ , it can be shown that the relationship between these quantities is given by:-

$$\tan \Psi = \tan \theta \sec \frac{\phi}{2} .$$

Hence since θ is known, 10^{o} in the case of the UK6 satellite, to calculate the sun to actual spin axis angle Ψ , it is only necessary to determine ϕ . This can conveniently be measured by using the null generated by the detector on a datum crossing of the slit to start a counter and noting its content at subsequent transits of the slit during one complete revolution of the satellite, Fig.4. Thus if n_1 is the count recorded at the second sun transit of the slit, and n_2 the count at the completion of one revolution:-

$$\phi = \frac{n_1}{n_2} 2\pi \quad \text{rad} .$$

In the case of the coning angle sensor two precision sun slit detectors are mounted orthogonally in the satellite so that the intersection of their fields of view is nominally coincident with the nominal spin axis of the vehicle, their actual direction in satellite coordinates being measured as accurately as may be required during assembly. Rotation of the satellite, as with the sun angle sensor, will again cause the sun to transit each of the slits twice in a single revolution of the vehicle. If no misalignment between the nominal and actual spin axis of the satellite exists, the angular separation of these transits will all be exactly 90^o independent of the sun to spin axis angle. If, however, the spin axis does not lie along the intersection of the two null detection planes of the sensor the angles depart from 90^o by an amount depending on both the angular misalignment θ_s and the sun to spin axis angle Ψ .

The components, measured by the two slits, of the misalignment angle θ_s are related to the sun to actual spin axis angle and satellite rotation required to produce successive sun transits of the two slits by the same relationship as that derived for the sun angle sensor.

Thus

$$\tan \Psi = \tan \theta_{s1} \sec \frac{\phi_1}{2}$$

$$\tan \Psi = \tan \theta_{s2} \sec \frac{\phi_2}{2}$$

or

$$\tan \theta_{s1} = \tan \Psi \cos \frac{\phi_1}{2}$$

$$\tan \theta_{s2} = \tan \Psi \cos \frac{\phi_2}{2}$$

where θ_{s1} and θ_{s2} are the components of the spin axis misalignment error θ_s , Ψ is the sun to spin axis angle determined by the sun angle sensor and ϕ_1, ϕ_2 are the angular rotations of the satellite required to cause successive crossings of each slit as shown in Fig.5. The satellite rotation angles ϕ_1 and ϕ_2 are again measured by using a counter started at a datum crossing of one of the slits and its value read out at each successive crossing during one complete revolution. Thus from Fig.5:-

$$\phi_1 = \left(\frac{n_4 - n_2}{n_4}\right)2\pi \quad \text{rad}$$

$$\phi_2 = \left(\frac{n_3 - n_1}{n_4}\right)2\pi \quad \text{rad} \quad .$$

Two restrictions on the sun to spin axis angle need to be noted:-

(a) If the sun to spin axis angle is less than the inclination of the slit for the sun angle sensor, or in the case of the coning angle sensor the misalignment between the actual and nominal spin axis of the satellite is greater than the sun to spin axis angle the sensors fail because the sun remains outside the field of view of the sensors.

(b) As the sun to spin axis angle approaches 90° the satellite rotation angles required for successive sun transits of the coning angle sensor tend to 90° independently of any misalignment that may exist.

4 ERROR ANALYSIS

In practice, imperfections in the geometry of the slits in both sensors will introduce errors in the measured values of ϕ , the satellite rotation angles required for successive sun transits of the detector slits. In addition, further errors will be introduced into the subsequent computation of the spin axis coning angle misalignment error, due to the uncertainty in the value of Ψ determined by the sun angle sensor. To obtain Ψ from this sensor a knowledge of θ , the inclination of the slit to the satellite spin axis, is required. The value of θ , which needs to be accurately known in cases where the sun angle sensor is used in isolation, can in the case where the sensor is used in a complementary fashion with the coning angle sensor, have an iterative correction process applied between the two sets of data to give progressively more accurate values for both θ_s and Ψ, starting with a nominal value for θ. This initial value of θ assumes that no misalignment exists between the nominal and actual spin axis of the vehicle.

The error dependency between the various parameters can easily be determined by differentiating the basic relationship:-

$$\tan \Psi = \tan \theta \sec \frac{\phi}{2} .$$

The relationship $\frac{\Delta\Psi}{\Delta\theta}$ against θ for two values of the slit inclination angle (10° and 15°) are given for the sun angle sensor in Fig.6. The ratio of $\frac{\Delta\Psi}{\Delta\theta}$ rising rapidly to a maximum value of 2.95 at a sun to spin axis angle $\Psi = 45^{\circ}$. Although the figure shows that errors in Ψ for a given error in θ become less as the slit inclination is increased, this can only be achieved at the expense of limiting the sun to spin axis angle at which the sensor can operate.

$\frac{\Delta\Psi}{\Delta\phi}$ as a function of ψ, that is the sensitivity of the sun to spin axis angle determined by the sun angle sensor to errors in the measured rotation of the satellite necessary to produce successive transits of the sun slit, is given in Fig.7. The maximum value of $\frac{\Delta\Psi}{\Delta\phi} = 2.3$ in this instance occurs at a sun to spin axis angle $\Psi = 90^{\circ}$. Again it can be seen that a reduction in the error relationship between $\Delta\Psi$ and $\Delta\phi$ can be achieved by increasing the slit to spin axis angle θ, providing the sun to satellite spin axis restriction as outlined above can be tolerated.

Similar relationships derived for the coning angle sensor showing the sensitivity of θ_s to errors in Ψ and ϕ as a function of sun to spin axis angle Ψ are shown in Fig.8 for a coning misalignment error of one degree.

Curve 1 which shows $\frac{\Delta\theta_s}{\Delta\Psi}$ to have a minimum value at $\Psi = 45^{\circ}$ can be seen to increase rapidly as Ψ tends to 0° or 90°, whereas curve 2, shows the sensor to be fairly tolerant of errors in ϕ, that is to errors in the slit geometry, for small angles of Ψ but to increase rapidly as ψ gets larger.

From these curves we can see that the errors will combine to have least effect if the sensor is operated close to the middle of its range, that is $\Psi = 45^{\circ}$, but in any case are unlikely to be serious anywhere over the anticipated working range for the sensor of $\Psi = 10^{\circ}$ to $\Psi = 80^{\circ}$.

5 TEST RESULTS

A coning angle sensor has been constructed in order to assess the performance of two prototype precision sun slits. The sensor was mounted on an adjustable plate which enabled various coning angles to be set relative to a drive shaft, the shaft being driven at 60rev/min by a synchronous motor which with refinements, gave the shaft, and hence sensor, an angular rotation with irregularities of less than one to two parts in 10^5, equivalent to an error of approximately 0.5°. The whole assembly was then mounted on a rotary table in front of a solar simulator thus allowing various values of Ψ to be obtained at which the set coning angle could be measured, Fig.9. A 20 bit counter was used, with a clock frequency of 131kHz to give a resolution for θ of about 10 seconds of arc per count.

The sensor, and thus precision sun slits, were assessed by setting a known coning angle for the sensor and comparing this with the angle derived by the sensor at various values of 'Ψ'. Because the diameter of the exit beam of the solar simulator was inadequate to fully illuminate both slits of the sensor, thus possibly introducing errors in the sensor output due to variations in the beam quality, two sets of results were taken for the same range of sun to spin axis angles, with the sensor translated into two different areas of the beam. About ten readings were made at each setting of 'Ψ' and the mean and standard deviation calculated; the results of these tests are shown in Fig.10.

These results, which were generally very satisfactory showing errors of less than 6 minutes of arc between the coning angle set and that determined by the sensor, do however indicate that significant errors are introduced due to inadequacies in the solar simulator, hence preventing the true sensor performance being established with the present test arrangement. A further programme of measurements is to be carried out on the sensors developed for the UK6 satellite, using the sun as a source of illumination, to establish the full sensor performance.

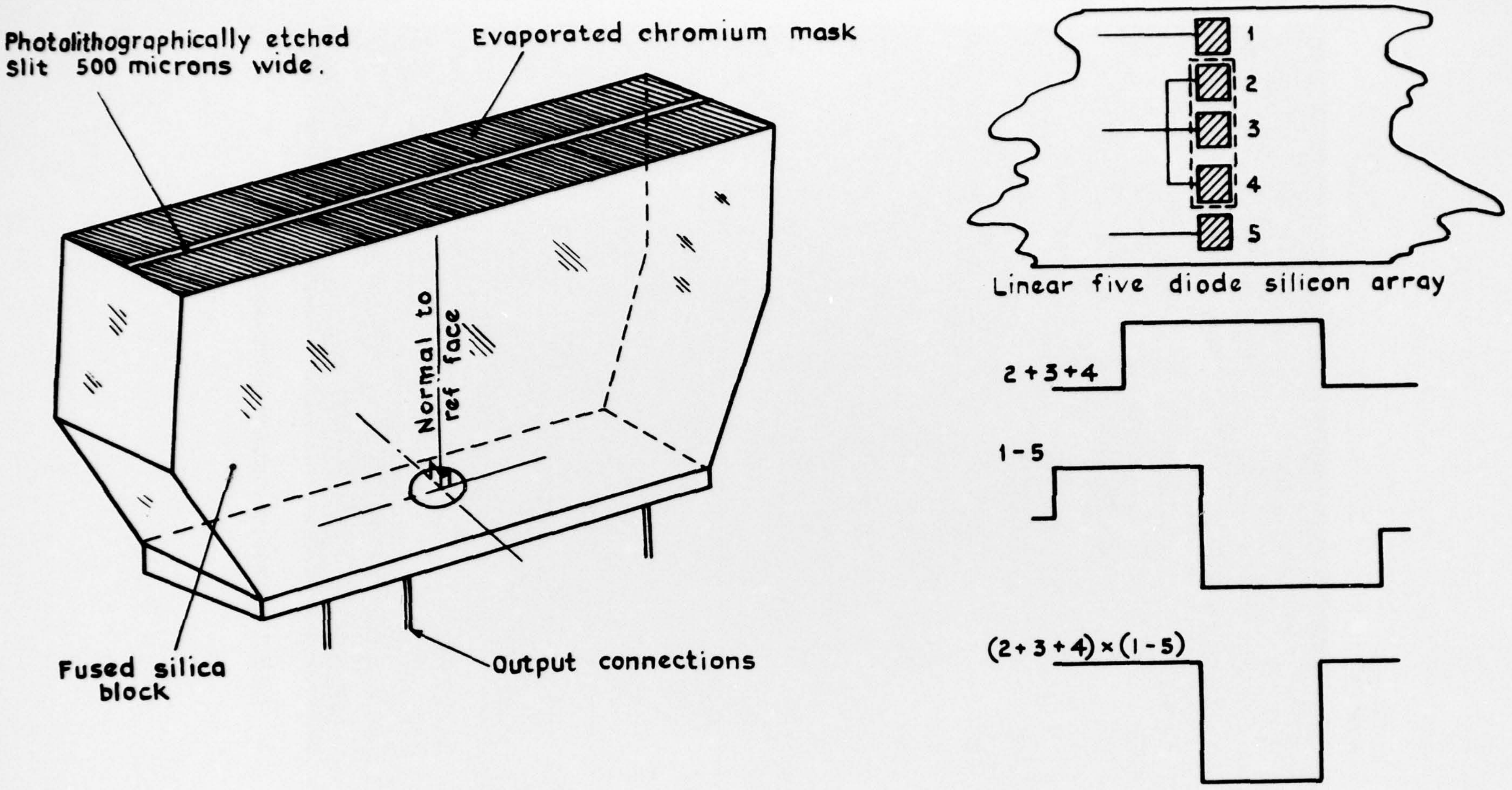

Fig.1 Precision sun slit detector

Fig.1

Fig.2

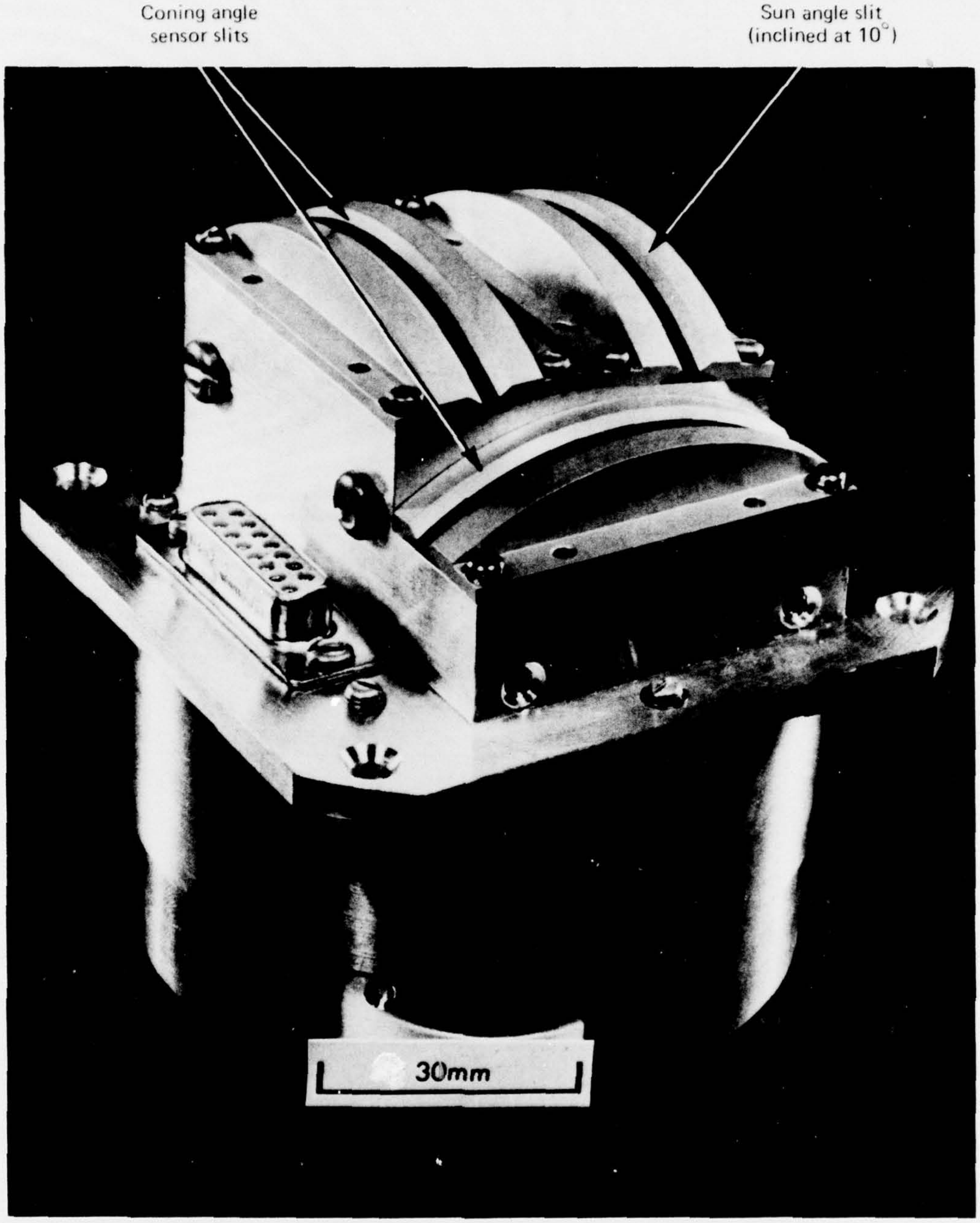

Fig.2 Combined sun angle and coning angle sensor

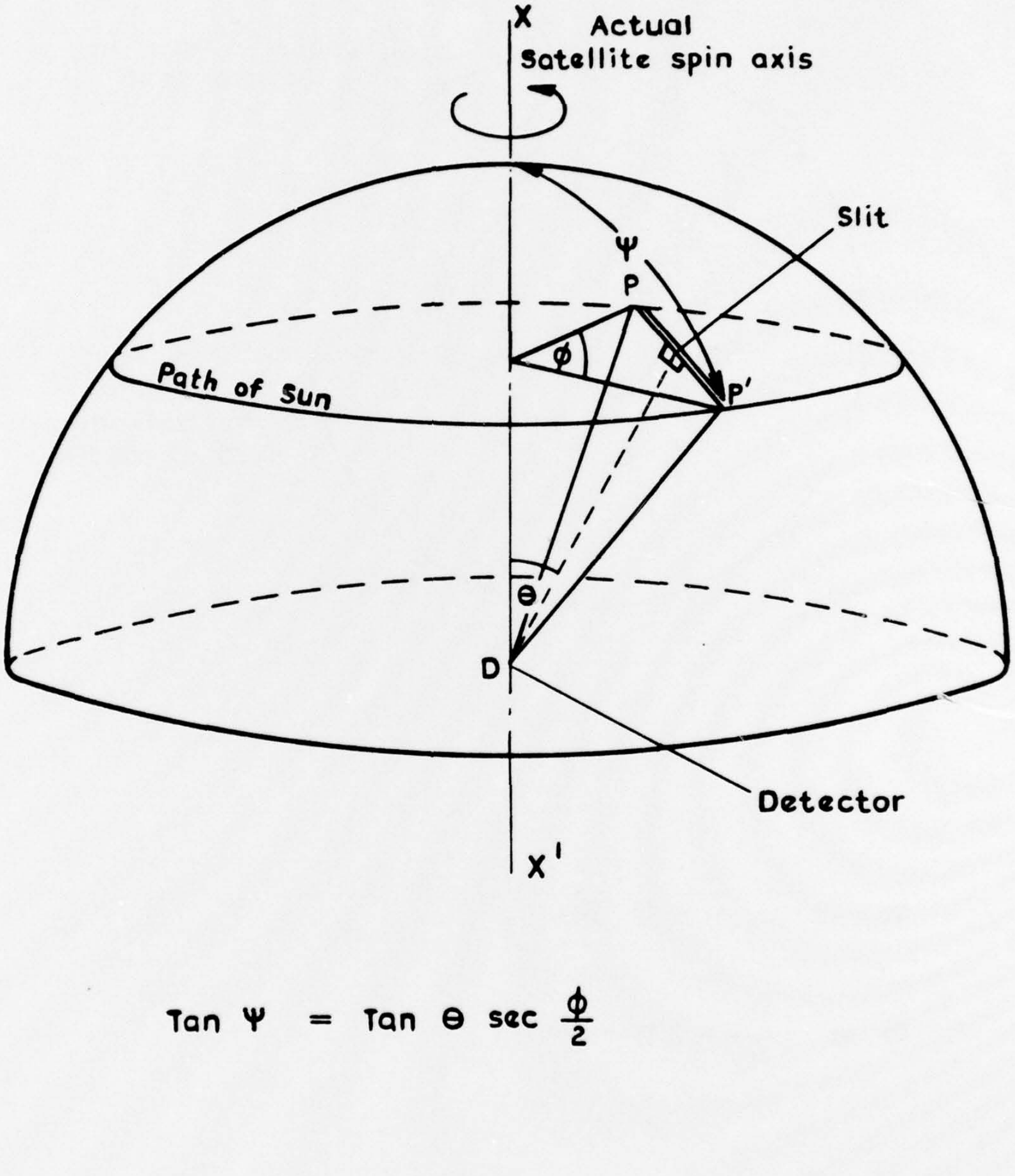

$$\tan \Psi = \tan \theta \sec \frac{\phi}{2}$$

Fig. 3 Geometry of inclined slit sensor

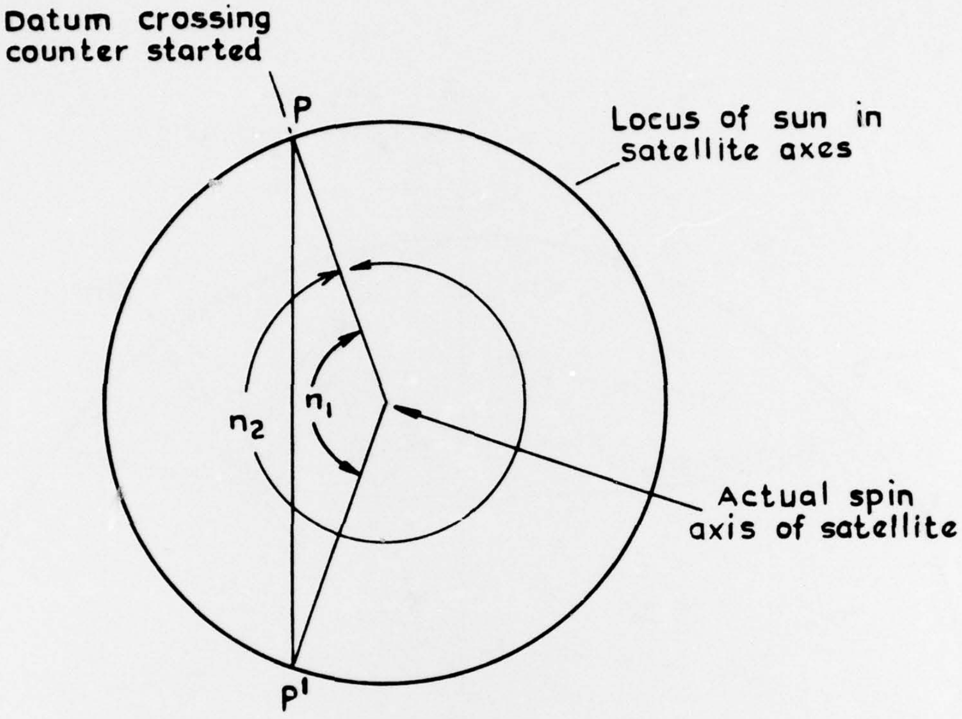

$$\tan \Psi = \tan \Theta \sec \frac{\phi}{2}$$

$$\phi = \frac{n_1}{n_2} \cdot 2\pi \text{ rads}$$

FIG. 4 Derivation of ϕ for sun angle sensor

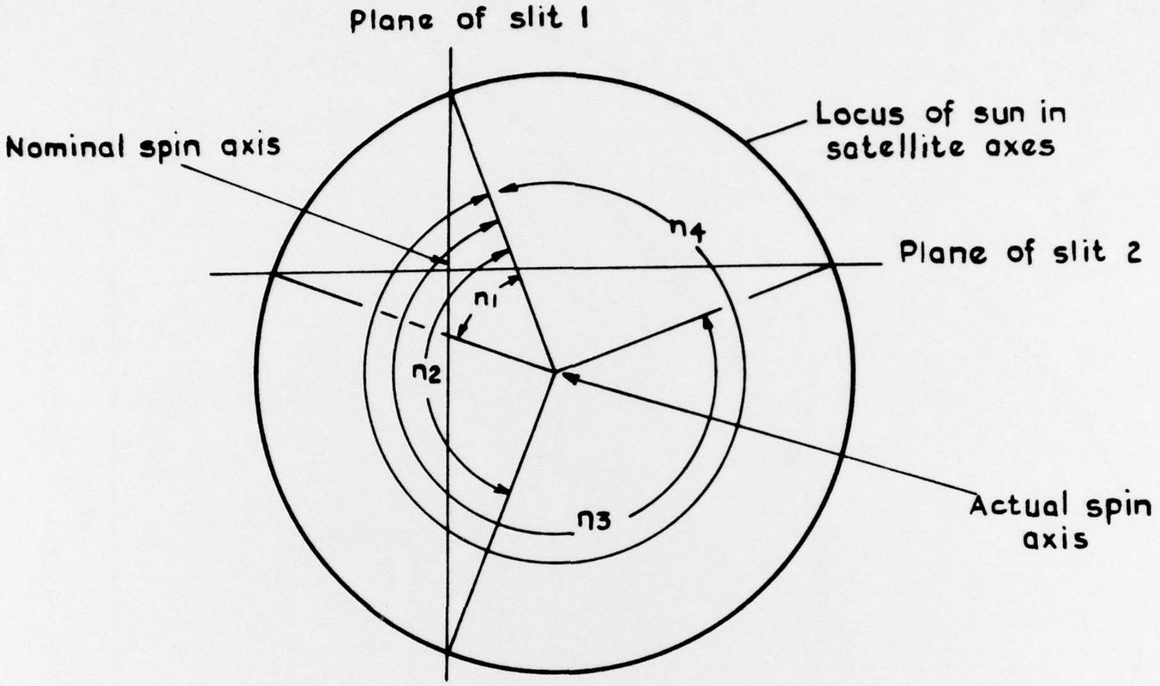

T.R. 76076

$$\phi_1 = \left(\frac{n_4 - n_2}{n_4}\right) \cdot 2\pi \text{ radians}$$

$$\phi_2 = \left(\frac{n_3 - n_1}{n_4}\right) \cdot 2\pi \text{ radians}$$

$$\operatorname{Tan} \theta_{s1} = \operatorname{Tan} \psi \cos \frac{\phi_1}{2}$$

$$\operatorname{Tan} O_{s2} = \operatorname{Tan} \psi \cos \frac{\phi_2}{2}$$

004 905902

Fig. 5 Derivation of ϕ_1 and ϕ_2 for coning angle sensor

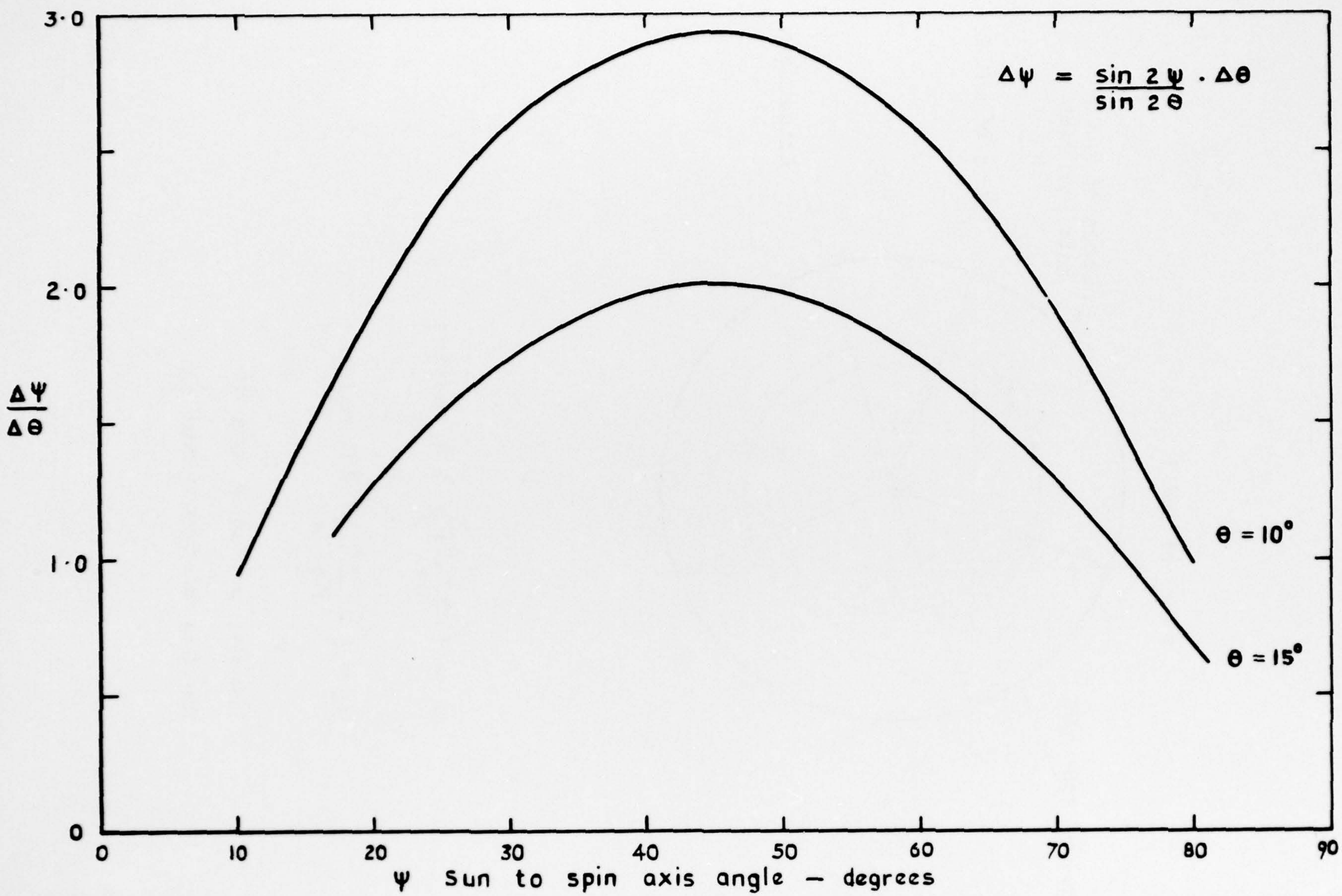

Fig. 6 Sun angle sensor error dependency of $\frac{\Delta\psi}{\Delta\theta}$ against ψ

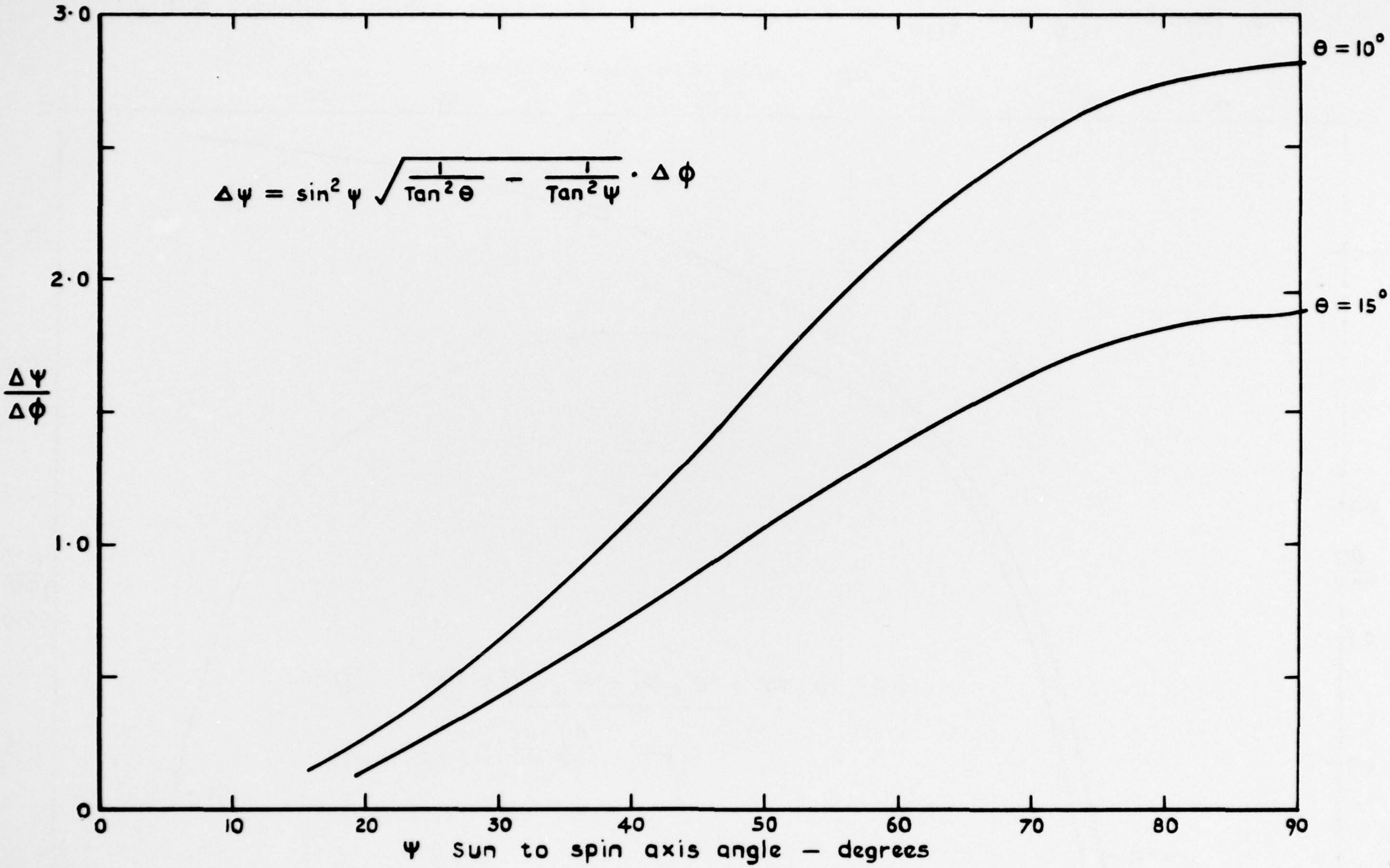

Fig. 7 Sun angle sensor error dependency of $\frac{\Delta\psi}{\Delta\phi}$ against ψ

Fig.7

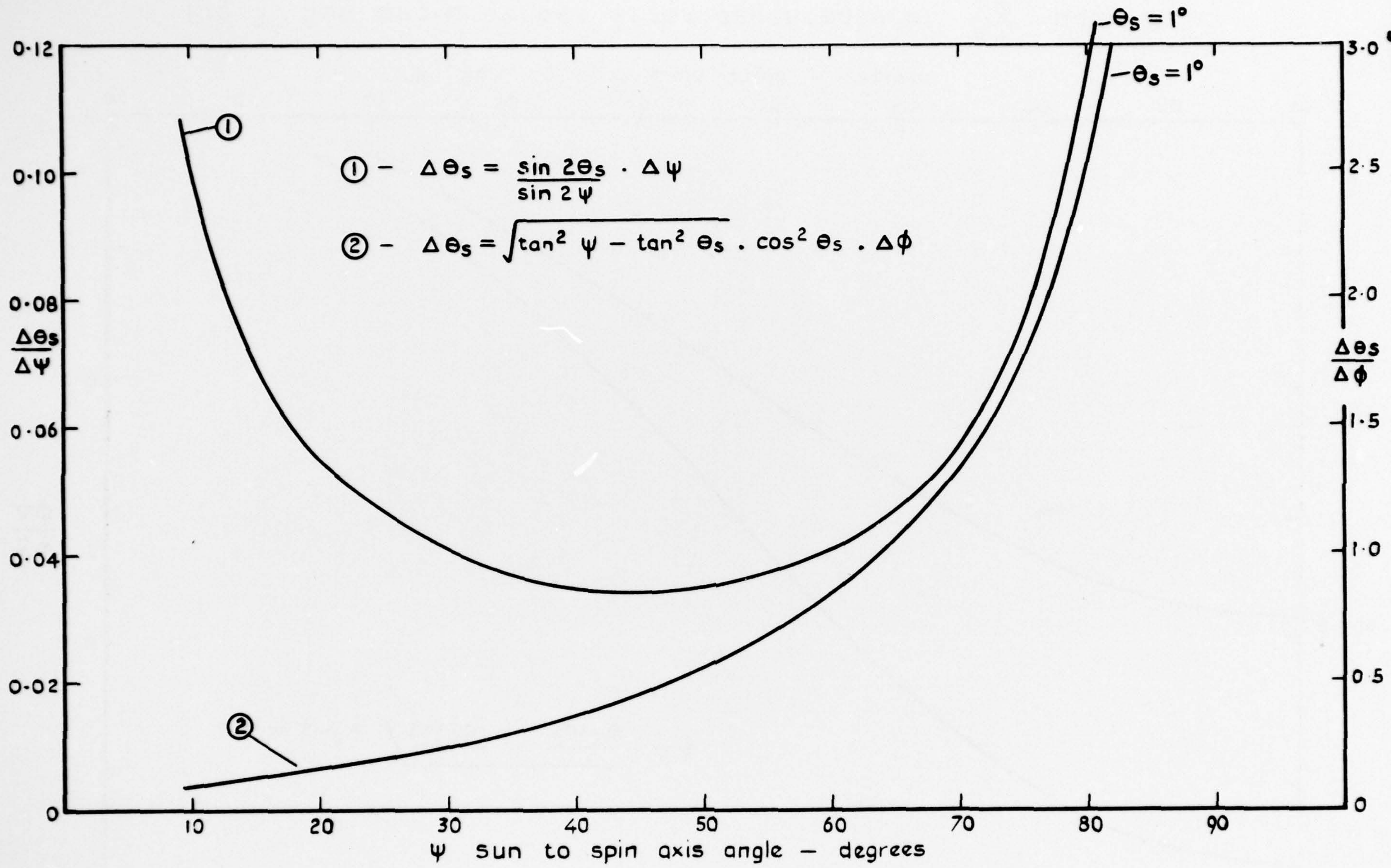

Fig. 8 Coning angle sensor error dependency of $\frac{\Delta\theta s}{\Delta\psi}$ and $\frac{\Delta\theta s}{\Delta\phi}$ against ψ

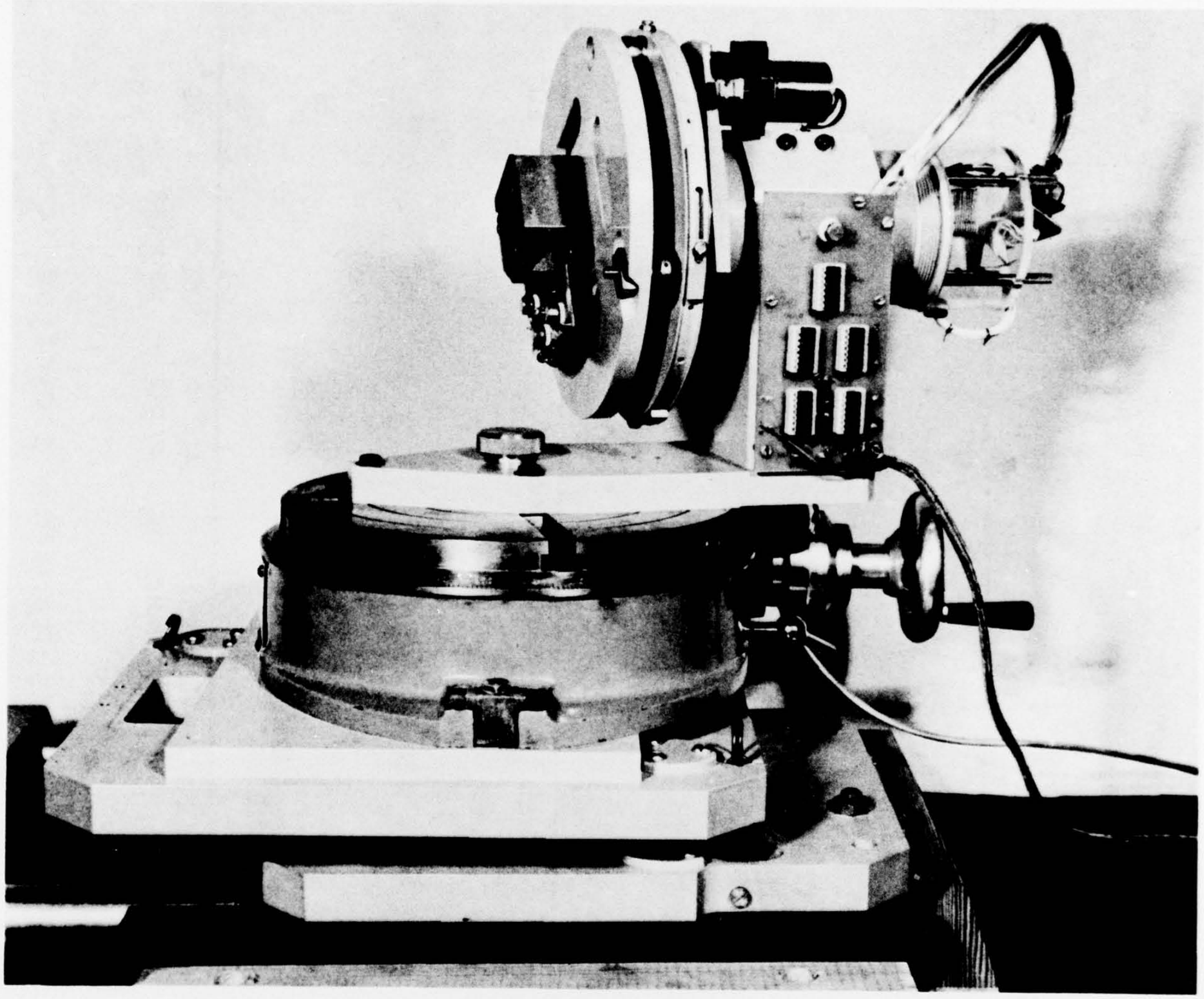

Fig.9 Coning angle sensor test rig

Fig.10

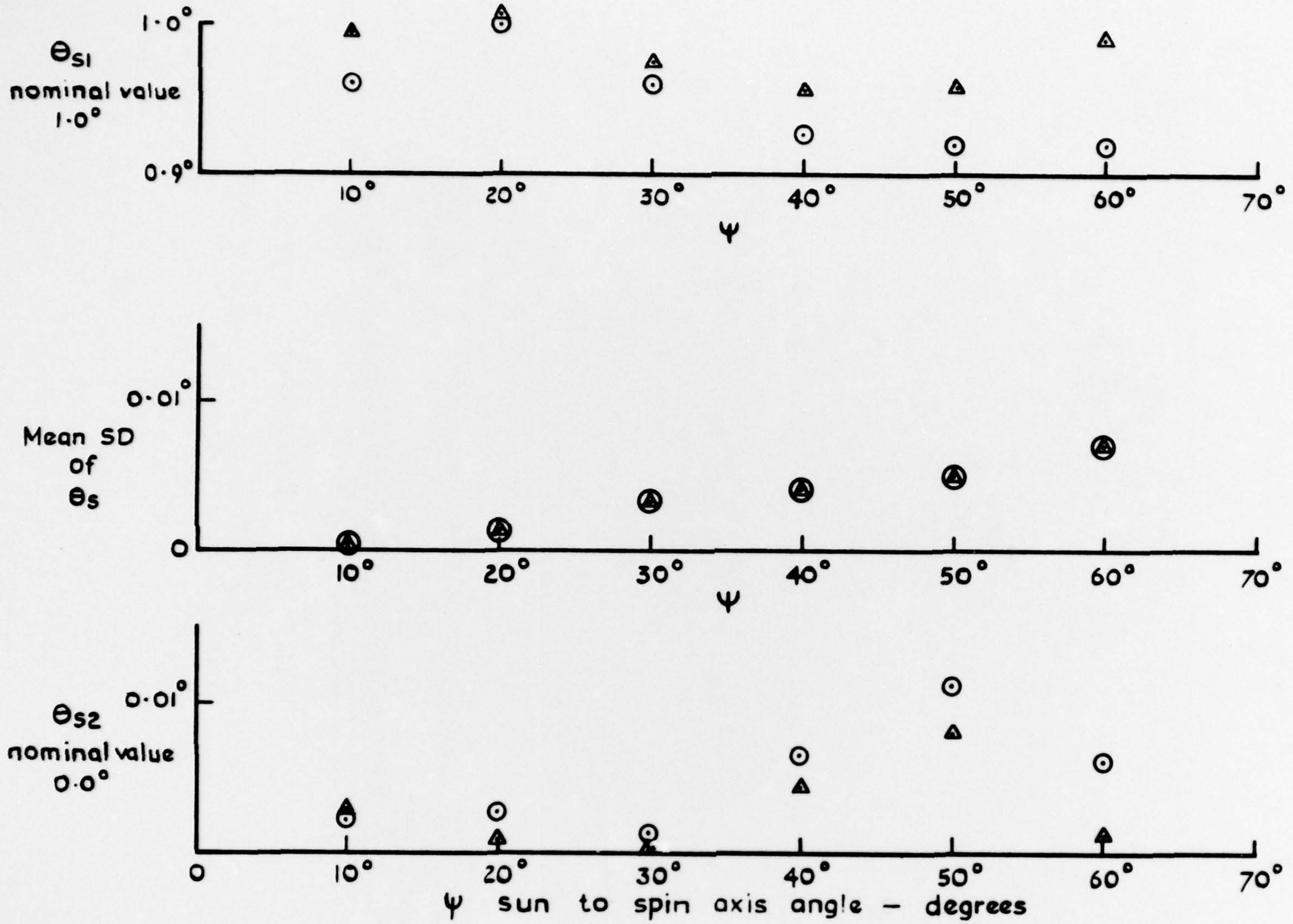

Fig. 10 Results from prototype sensor